JOURNAL OF MATERIALS SCIENCE 31 (1996) 3723–3729

Stresses and failure in the diametral compression test

M. K. FAHAD
Industrial Research Laboratories, University of Durham, UK

The validity of the diametral disc test with a small flat ground has been established. The stress distribution was determined by a finite element method for a range of loading conditions. The results show that for the case of a point load, the failure is due to shear and compressive stresses at the loading point. Application of the diametral disc test for a ground flat was proposed and tested. The width of the flattened area must be less than 0.2 times the diameter of the disc to obtain accurate tensile strength.

1. Introduction

The diametral compression test, the Brazilian test, and the indirect tensile test are three names for one test method that has been used to measure the tensile strength of concrete [1]. It has also been used to measure the tensile strength of rock [2], coal [3], polymers [4], cemented carbides [5], and ceramics [6–8]. The test was independently introduced by Carniero and Barcellos [9] in Brazil, and Akazawa [10] in Japan, around 1953. The diametral compression test was based on the fact that tensile stresses developed when a circular disc was compressed between two diametrically opposed forces. The maximum tensile stresses grow perpendicularly to the loading direction and are proportional to the applied load.

The most important thing to note about diametral disc testing is that fracture must be initiated by tensile stresses if the test is to yield useful results. Because failure occurs along the diametral plane of the applied load, it is commonly assumed that the nominal tensile stress causes the disc to fail. However, some researchers [11, 12] believed that failure is initiated under the load points. Because of this there is some disagreement as to what exactly is the mechanism of failure.

Takagi and Shaw [13] proposed that plastic flow occurred before fracture and that the material becomes plastic near the applied load before becoming plastic at the centre of the disc. As a result, the intensified tensile stresses at the centre will be greater than at any other point towards the applied load. Therefore, failure is initiated at the centre of the disc. This was proved by Sampath and Shaw [14] using a very thin crack gauge (300 μm gold film).

In fact, the strength values obtained in diametral compression testing are always much lower than for other uniaxial tests, such as three- and four-point bending. Wright [1] suggested many reasons for these differences. The first explanation was that the formula used for computing the tensile strength from the load is assumed to follow Hooke's law. But many brittle materials, such as concrete, do not follow Hooke's law exactly. The second reason may be the specimen size effect. Whereby the statistical theory of brittle fracture predicts a decrease in the average strength with an increase in the specimen volume under tensile stress. The third reason suggested by Wright is that brittle materials obey the maximum tensile strain criterion. Therefore, in the case of three- or four-point bending, there are only tensile stresses at the point of fracture. However, in the diametral disc test, the centre of disc is subjected to a compressive stress perpendicular to the tensile stress and the strain produced by the two stresses are in the same direction.

The objective of the present work was to investigate the validity and the point of fracture initiation of the diametral compression test.

2. Stress analysis

A theoretical basis for the stress analysis of a disc subjected to two concentrated diametral forces, has been postulated by Timoshenko and Goodier [15] and by Frocht [16]. This can be seen in Fig. 1a. Frocht also illustrated that the stress state at any point within, and on, the disc can be calculated [16] by using three general equations

$$\sigma_x = \frac{2P}{\pi Dt} - \frac{2P}{\pi t}\left\{\frac{x^2(R-y)}{[x^2+(R-y)^2]^2} + \frac{x^2(R+y)}{[x+(R+y)^2]^2}\right\} \quad (1)$$

$$\sigma_y = \frac{-2P}{\pi Dt} - \frac{2P}{\pi t}\left\{\frac{(R-y)^3}{[x^2+(R-y)^2]^2} + \frac{x^2(R+y)^3}{[x^2+(R+y)^2]^2}\right\} \quad (2)$$

$$\tau_{xy} = \frac{2P}{\pi t}\left\{\frac{x(R-y)^2}{[x^2+(R-y)^2]^2} - \frac{x(R+y)^2}{[x^2+(R+y)^2]^2}\right\} \quad (3)$$

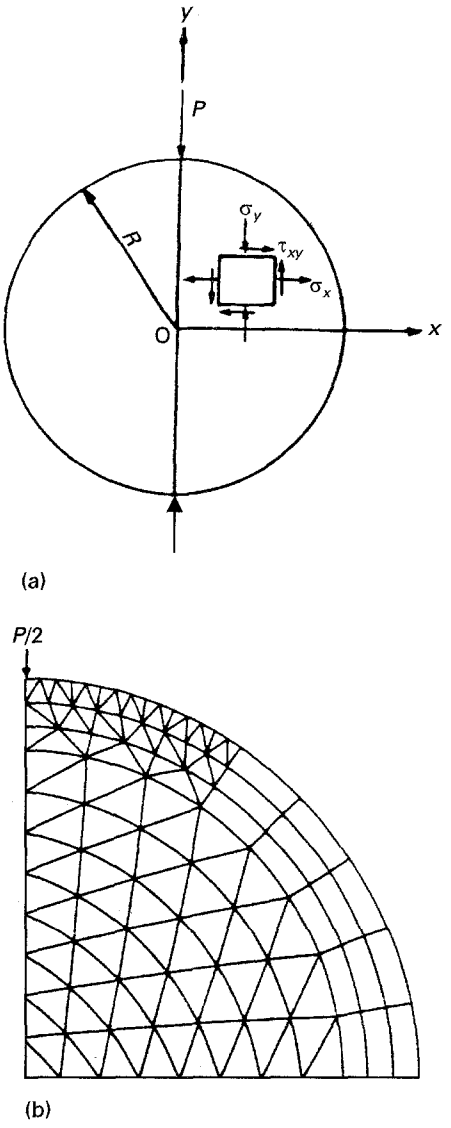

Figure 1 The diametral disc test under point load. (a) Geometry and notations, (b) finite element mesh.

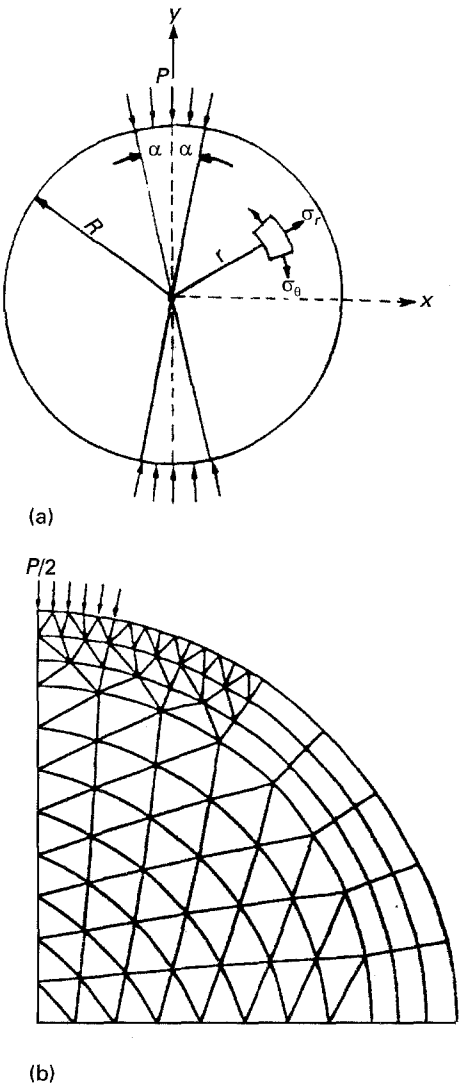

Figure 2 The diametral disc test under distributed load. (a) Geometry and notations, (b) finite element mesh.

where P is the applied load, t the thickness of the disc, D the diameter, R the radius of the disc, σ_x and σ_y are normal stresses in the directions perpendicular and parallel, respectively, to the loaded diameter, and τ_{xy} is the shear stress; Fig. 1. The above equations show that along the loaded diameter ($x = 0$), the normal stress, σ_x, is tensile and constant with magnitude equal to

$$\sigma_x = 2P/\pi Dt \tag{4}$$

σ_y, parallel to the loaded diameter is a compressive stress. This increases from $3\sigma_x$ at the centre of disc to infinity beneath the loading points. The shear stress, τ_{xy} is zero along the diameter plane and hence σ_x and σ_y are the principal stresses on the plane.

Although the above equations assume a point load on a thin disc, in practice the load is distributed over a finite area. Therefore, the above equations must be modified to reflect the finite load distribution. Hondros [17] developed an exact theoretical stress analysis for the case of a pressure applied over two diametrically opposite arcs of angular width 2α as shown in Fig. 2. He showed that the stresses along the Y-axis are described by the following equations

$$\sigma_{\theta y} = \frac{2p}{\pi}\left\{\frac{(1 - r^2/R^2)\sin 2\alpha}{1 - 2(r^2/R^2)\cos 2\alpha + r^4/R^4} - \tan^{-1}\left[\frac{(1 + r^2/R^2)}{(1 - r^2/R^2)}\right]\tan\alpha\right\} \tag{5}$$

$$\sigma_{ry} = \frac{-2p}{\pi}\left\{\frac{(1 - r^2/R^2)\sin 2\alpha}{1 - 2(r^2/R^2)\cos 2\alpha + r^4/R^4} + \tan^{-1}\left[\frac{(1 + r^2/R^2)}{(1 - r^2/R^2)}\right]\tan\alpha\right\} \tag{6}$$

where p is applied pressure and α is a small angle defined in Fig. 2, R is the radius of the disc. Inspection of above equations that the maximum compressive stress at the point of applied load is finite, instead of an infinite as when using Equation 2. Also Equations 5 and 6 yield identical stresses at the centre of disc, given by point loads, P, applied at the ends of the diameter as shown below.

When substituting $r = 0$ (at the centre of disc), Equation 5 becomes

$$\sigma_{\theta y} = \frac{2p}{\pi}(\sin 2\alpha - \alpha) \tag{7}$$

When α is small, $\sin 2\alpha \approx 2\alpha$, $P = p\alpha Dt$ and Equation 7 becomes

$$\sigma_{\theta y} = \frac{2p\alpha}{\pi} = \frac{2P}{\pi Dt} \tag{8}$$

A number of years ago, the finite element method was used to analyse the stress distribution of a diametral disc test [18]. This analysis was in good agreement with the analysis of Frocht [16] who used photoelastic techniques especially at the centre of the disc. Price and Murray [4] also analysed the diametral compression test using the finite element method. They pointed out that the finite element method gave a good result compared with a photoelastic stress distribution and with stresses calculated by an elasticity solution for a point near the centre of the disc.

3. A new analysis of the diametral compression test

Although there is a complete analytical solution for the diametral disc test, it was considered that the effects of a flat ground on opposite sides could be significant on the stress distribution. Therefore, finite element methods have been used to study the stress distribution of the diametral compression test.

3.1. Mesh design

The symmetry of the system enables the problem to be solved from analysis of the four quarters of the discs as shown in Fig. 1b. The diameter of the disc chosen was five times larger than the thickness to ensure that the analysis just included plane stresses [19]. The element and mesh used to analyse the disc segment are shown in Fig. 1. To reduce the error in evaluating stresses in the vicinity of applied load, mesh refinement is carried out only at the region of applied load.

3.2. Stress analysis for the point load case

The load in this case was applied at only one point, shown in Fig. 1b. Finite element methods indicate that for this type of loading there is a good agreement between the theoretical solution of Frocht [16] and finite element calculations, see Fig. 3. The tensile stress, σ_x, at the centre of disc was three times as large as the compressive stress. The tensile stress is constant along the loaded diameter, however, it rose sharply in the boundary regions between the tensile and compressive stresses. This may be attributed to the uncertainty of the finite element method beneath the load. In the y direction, only compressive stresses exist and the magnitude becomes very high beneath the load,

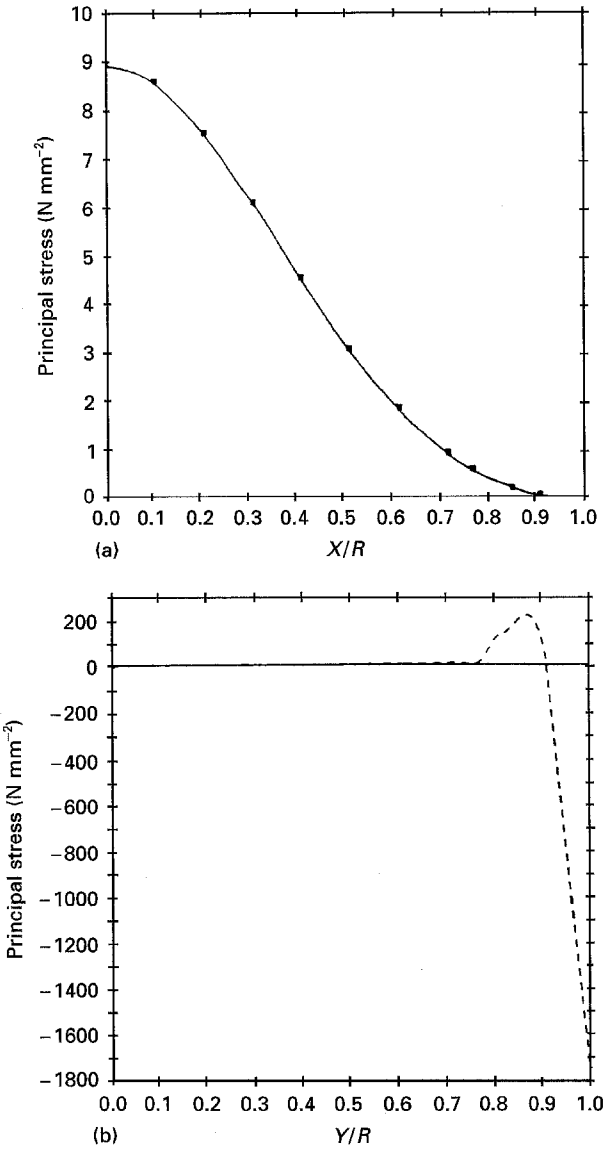

Figure 3 Principal stresses along the (a) x and (b) y axes for a point load diametral disc test. (——) Forch analysis, (– – –) or (×) finite element.

up to a hundred times the tensile stress at the centre of disc. Because of these higher compressive stresses, failure may be initiated at this region rather than at the centre. For this reason, point loading is not recommended.

3.3. Stress analysis for the distributed load case

As discussed in the preceding section, the specimen may fail at the load regions due to the compressive and shear stresses and not in the central part of the specimen due to the tensile stress. It was found that a distributed load applied over a finite area will reduce any stress concentration and consequently prevent the compressive and shear failure at the load region. One method used to distribute the load was by placing packing strips (shims) of suitable material between the specimen and the loading platens. However, care should be taken in choosing the shims for different test materials. Rudnick *et al.* [20] found that the strength values obtained are a function of the shim materials

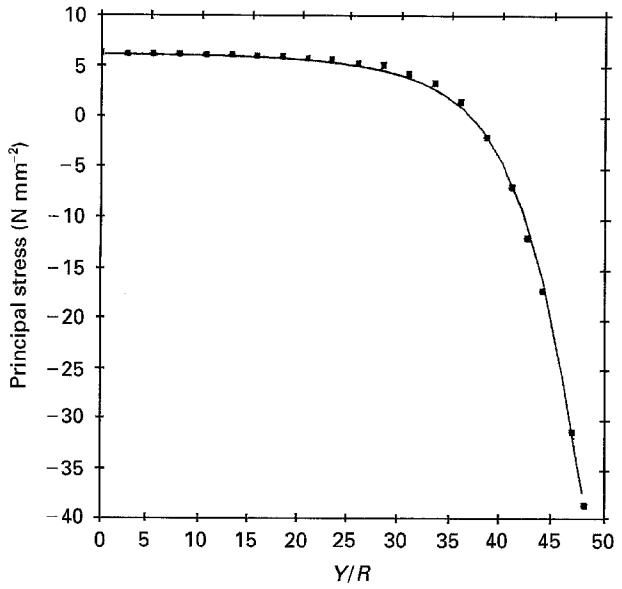

Figure 4 Variation of the tensile stress along the Y-axis for the diametral disc test under distributed load, (——) Hondros' equation, (■) finite element.

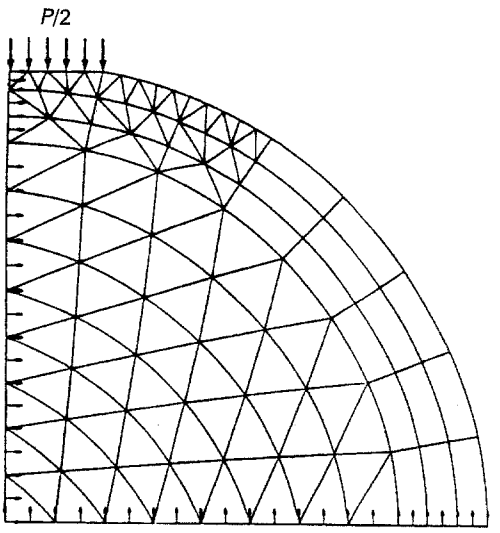

Figure 5 Finite element mesh for quartrant of a disc with a flat surface.

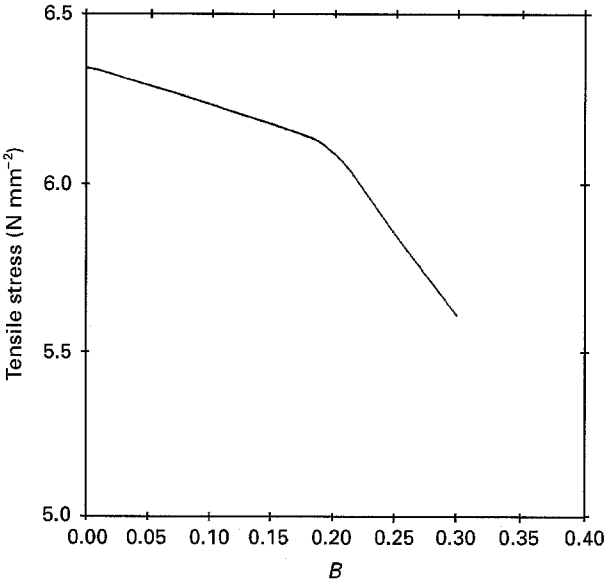

Figure 6 The effect of the flat surface area on the tensile stress at the centre of the diametral disc test.

used. Therefore, much experimental work was needed to choose the correct material shims. Alternative ways of distributing the load are examined below.

3.3.1. Curve distributed load

For this case, the load was distributed over a small arc of finite width instead of a point, see Fig. 2. Hondros [17] has developed an exact theoretical stress analysis for this case. The stress analysis was carried out using finite element methods to review the effect of using small arcs upon the stress distribution of the disc. The results of the principal stress distributions are shown in Fig. 4 for an angle of $\alpha = 11.45°$. Compared with the theoretical case, a good correlation exists between the Hondros solution and the finite element method. As expected, the compressive stresses beneath the arc loading decreased as the arc increased; for example, in this case, it was found that the compressive stress beneath the load was 8.40 times the tensile stress at the centre of the disc. Although compression failure may not be initiated with arc loading, it is difficult to perform this type of loading. This is because the load may not be uniformly distributed over the area of contact between the arc anvils and the specimen circumference.

3.3.2. Flat distribution load

One other method of loading the disc, is by flattening the disc over the loading area. This method avoids local crushing. The difference between this type of loading and the arc loading case is that the latter has an exact stress analysis given by Hondros [17], while the former has not.

In order to see more clearly the effect of the flat surfaces over the distributed stresses on the disc, the finite element method, see Fig. 5, has been used to analyse the stress distribution for this case. The investigation has been carried out for different load area widths, B, namely, 0.15, 0.2 and 0.3 times the diameter of the disc specimen. Finite element calculations show that an increase in B results in a decrease in σ_x at the centre of the disc, see Fig. 6, and leaves the compressive stresses at the centre virtually unaffected. Consequently, the stress ratio (σ_y/σ_x) increases at the centre of the disc. It may also be seen from Fig. 6 that the tensile stress, σ_x, varies little with change in B for the flat area in $0 < B > 0.2D$. Consequently, the error produced by using Equation 4 is also small (4%). However, in cases where $B > 0.2D$ the tensile stresses at the centre of the disc fell rapidly and no longer agreed with those given in Equation 4. Furthermore, finite element techniques demonstrate that the stress distribution in the flattened disc case is essentially identical to the case where an arc was used.

4. Experimental procedure

All test specimens used in this work were prepared from plaster of paris using silicon-rubber moulds. Plaster of Paris was chosen because it satisfactorily behaves like a typical brittle material, and is easily available and fabricated.

All specimens were prepared using a water/plaster ratio of 50/100. This ratio was chosen because it gives stronger plaster [21]. To eliminate as far as possible the porosity due to entrapped air, the slurry had to be mixed in a vacuum. It was necessary to fill the mould and level out the plaster using a spatula within 4 min. This is because the slurry becomes unworkable after that time. The slurry was then poured into the mould which was placed on a vibrating bed in order to extract the last of the air bubbles in the slurry. The specimens were then removed from the mould and allowed to dry at room temperature in the open air for 28 days.

To perform all the tests under plane stress conditions and to decrease the non-uniform axial distribution of applied load, all the discs used in this work have a thickness of no more than one quarter of its diameter. It is worth pointing out that very thin discs should be avoided because they require very accurate alignment.

5. Results and discussion

5.1. Effect of ground flats

Three types of applied load were used to study the effect of the flat surfaces on strength and fracture. These are the point load, 0.2D and 0.3D flat ground. For each case, 15 specimens were tested. The results are tabulated in Table I, using nominal stress, $\sigma_1 = 2P/\pi Dt$, which refers to the individual test situation. It can be seen that the average tensile strength obtained from the point load case was significantly lower (33%) than the average tensile strength obtained from the other two flat cases.

The crack pattern produced from the point load tests is shown in Fig. 7c. It can be seen that the central fracture crack deflects at 45° at the loading point, which agrees very well with maximum shear stresses. Fig. 8 demonstrates another benefit of the use of the

TABLE I The diametral disc test results for $D = 40$ mm and $t = 10$ mm

Rank	Nominal stress (MPa) for $D = 40$ mm, $t = 10$ mm		
	$B = 0$	$B = 0.2D$	$B = 0.3D$
1	3.19	4.21	5.38
2	3.20	4.28	5.56
3	3.21	4.31	5.86
4	3.31	4.73	6.06
5	3.35	4.81	6.15
6	3.38	4.97	6.41
7	3.39	4.98	6.45
8	3.50	5.03	6.50
9	3.52	5.12	6.60
10	3.77	5.24	6.66
Mean	3.38	4.76	6.16

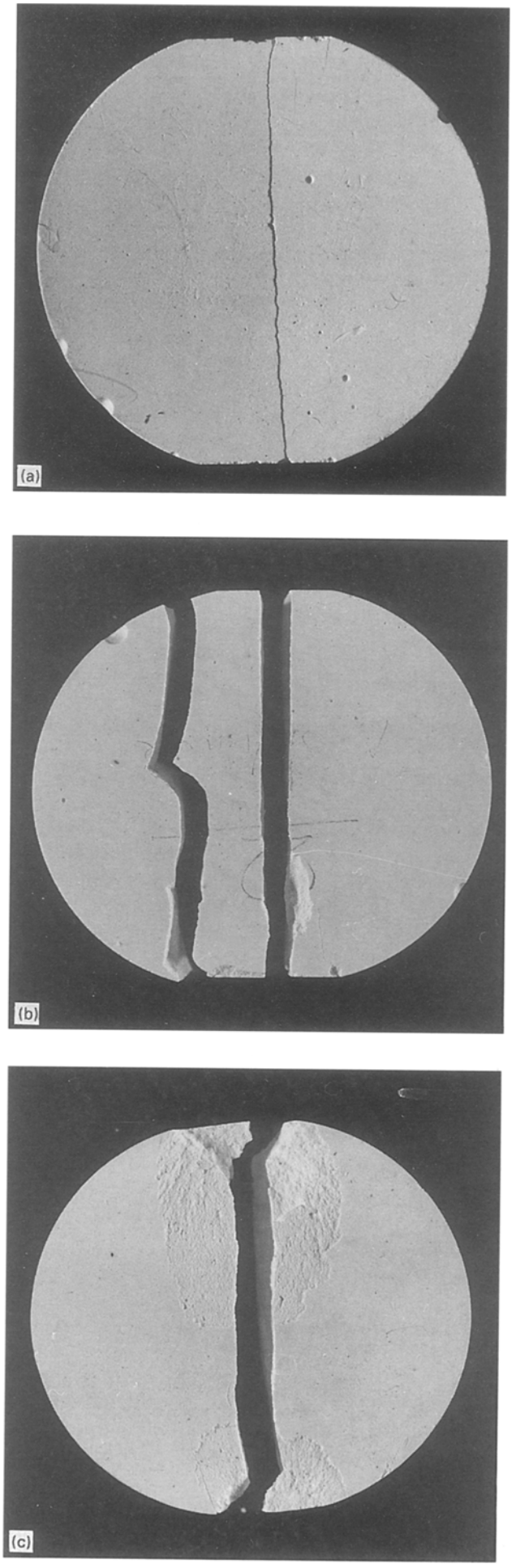

Figure 7 Typical fracture modes for diametral disc test. (a) Tensile fracture, (b) triple-cleft fracture, (c) point load fracture.

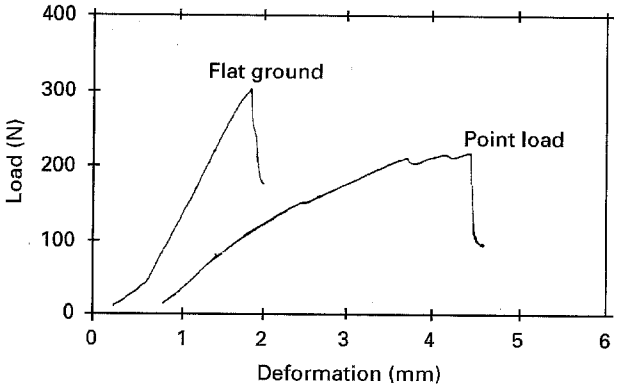

Figure 8 Load–deformation relationship for the diametral disc test.

flat surfaces. As can be seen, when flattened discs are used, the load–deformation curves show a linear relationship up to fracture. In comparison, the point load cases show non-linearity. At present it is believed that the failure of the point load case starts when shear cracks form at the edge of the loaded area due to the higher shear and compressive stresses. These propagate further by the action of the tensile stresses. As a result the tensile strength computed from this type of loading using Equation 4 is incorrect.

The results also show that the 0.3*D* flat surfaces disc were stronger than 0.2*D* flat disc. This difference, however, is expected and confirmed by the finite element stress analysis in Section 3.3. This analysis showed that the tensile stresses at the centre of the disc reduced with increase of the flat surface area, see Fig. 6. Therefore, Equation 4 should not be used to calculate the tensile strength of 0.3*D* case. These results show that for the determination of the tensile strength of brittle materials, the width of the loading area, *B*, must not be larger than 0.2 times the diameter of the disc specimen.

Fig. 7 shows the more frequent modes of fracture for each case of loading. It was found that for both the 0.2*D* and 0.3*D* flat surfaces cases, the fracture propagates along the loaded diameter with very straight cracks which do not run the whole length of the disc diameter, see Fig. 7a. This is evidence that there is no failure near the loading point. In addition to tensile failures, the triple-fracture pattern occurred frequently. The triple-cleft fracture, see Fig. 7b, results from a secondary fracture initiated due to the bending of the two separate half-discs.

5.2. Effect of size

Two specimen sizes, 40 mm × 10 mm and 50 mm × 10 mm, were used to investigate the effect of size on the tensile strength of plaster. In addition to size effects, two types of loading conditions (point and 0.2*D* flat) have been carried out to study the effects of each parameter.

The tensile strengths were calculated using Equation 4. The results, including the average and standard deviation, are given in Table II. It can be seen that when the flattened discs are used, the smaller specimen size gives higher average tensile strengths compared with the larger one. These results agree with the statistical theories of brittle fracture. On other hand, in the case of point loads applied to the larger specimen size, slightly higher average tensile strengths were found, compared with the smaller disc. This higher average strength of the larger specimen is incompatible with the statistical theory of fracture. Ovri and Davies [6] reported similar results in testing silicon nitride discs using point loads. The authors believed that these discrepancies can be explained as follows: the point load case failure will not be tensile failure which may be due to higher shear and compressive stresses at the point of contact of the specimen and the loading platen. Therefore, an increase in the specimen volume under tensile stress will not affect the results.

TABLE II The diametral disc test results for $D = 50$ mm, $t = 10$ mm

Rank	Nominal stress (MPa) for $D = 50$ mm, $t = 10$ mm	
	$B = 0$	$B = 0.2D$
1	3.18	3.86
2	3.18	3.86
3	3.23	3.98
4	3.33	4.07
5	3.42	4.15
6	3.56	4.17
7	3.63	4.29
8	3.69	4.31
9	3.72	4.34
10	3.75	4.40
Mean	3.47	4.14

6. Conclusion

The diametral compression test has been evaluated and confirmed as a simple way of measuring the tensile strength of brittle materials. However, care must be taken when considering the results obtained from this test. In previous work, a number of authors have assumed that the disc specimen failed at the centre. This may not always be the case. Indeed, for the materials employed in this investigation, for the case of point load, it has been shown that the failure in the diametral compression test is due to shear and compressive stresses at the loading points. A different approach to the diametral compressive test with a ground flat has therefore been proposed and tested. The width of the flattened area must be approximately 0.2 times the diameter of the disc to obtain an accurate tensile strength. When discs with the appropriate size of the flattened area were used in tests, results were obtained which were consistent and in agreement with theories of brittle failure regarding the effects of specimen size.

References

1. P. J. F. WRIGHT, *Mag. Concr. Res.* July (1955) 87.
2. J. C. JAEGER and E. R. HOSKINS, *J. Geophy. Res.* **71** (1966) 2651.
3. R. BERENBAUM and I. BRODIE, *Br. J. Appl. Phys.* **10** (1959) 281.

4. H. L. PRICE and K. H. MURRAY, *J. Eng. Mater. Tech.* July (1973) 186.
5. M. C. SHAW, P. M. BRAIDEN and G. J. DESALVO, *J. Eng. Ind.* **96** (1975) 77.
6. J. E. O. OVRI and T. J. DAVIES, *Mater. Sci. Eng.* **96** (1987) 109.
7. R. M. SPRIGGS and L. A. BRISSETTE and T. VASILOS, *Mater. Res. Stand.* May **4** (1964) 218.
8. R. H. MARION and K. JOHNSTONE, *Am. Ceram. Soc. Bull.* **56** (1977) 998.
9. F. L. L. B. CARNIERO and A. BARCELLOS, "Concrete tensile strength", Union of Testing and Research Laboratories for materials and structures, Paris. No. 13 (1953).
10. T. AKAZAWA, "Tension test method for concrete", International Association of Testing and Research Laboratories for materials and structures, Paris, No. 16 (1953).
11. J. A. HOOPER, *J. Mech. Phys. Solids* **19** (1971) 179.
12. J. A. HUDSONN, E. T. BROWN and F. RUMMEL, *Int. J. Rock Mech. Min. Sci.* **9** (1972) 241.
13. J. TAKAGI and M. C. SHAW, *Ann. CIRP* **30**(1) (1981) 53.
14. W. S. SAMPATH, T. C. RAMARAJ and M. C. SHAW, Special volume published by ASME, Winter annual meeting, November, (ASME, 1985) p. 21.
15. S. P. TIMOSHENKO and J. N. GOODIER, "Theory of elasticity" (McGraw-Hill, New York, 1970).
16. M. M. FROCHT, "Photoelasticity" (John Wiley & Sons, New York, 1947).
17. G. HONDROS, *Aust. J. Appl. Sci.* **10** (1959) 243.
18. E. USUI, T. IHARA and T. SHIRAKASHI, *Bull. Jpn. Soc. Prec. Eng.* **13** (1979) 189.
19. P. M. BRAIDEN, Technical Paper MR73-916 (Society of Manufacturing Engineers, Michigan, USA, 1974).
20. A. RUDNICK, A. R. HUNTER and F. C. HOLDEN, *Mater. Res. Stand.* **3** (1963) 283.
21. J. J. RUSSELL and F. A. BLAKEY, *Aust. Appl. Sci.* **4** (1956) 175.

Received 12 May
and accepted 1 December 1995